E.A. ELISEEV

Institute for Problems of Materials Science, Nat. Acad. of Sci. of Ukraine
(3, Krzhizhanovs'kyi Str., Kyiv 03142, Ukraine; e-mail: eugene.a.eliseev@gmail.com)

PACS 77.80.Dj

THE STRUCTURE OF A 180-DEGREE DOMAIN WALL NEAR THE SURFACE OF FERROICS

We consider the influence of a built-in surface field on the 180-degree domain wall profile in primary ferroics within the Landau–Ginsburg–Devonshire phenomenological approach. The built-in surface field can be caused by various physical mechanisms for ferroelastic, ferroelectric, and antiferromagnetic media. For instance, it can be a component of the intrinsic surface stress tensor for ferroelastics with order parameter as a component of the strain tensor. We predict the effect of domain wall bending near the surface caused by the built-in field and derived the corresponding approximate analytical expressions.

K e y w o r d s: ferroics, phenomenological approach, domain wall bending, built-in surface field.

1. Introduction

The polarization structure at domain walls in ferroelectrics has been of permanent interest for fundamental science since the middle of the last century, starting from the earlier studies of Ising-like walls in uniaxial ferroelectrics, toward recent works, which focus attention on the mixed Ising–Bloch–Néel polarization structure of the walls encountered in multiaxial ferroelectrics and multiferroics (see, e.g., [1–4] and references therein). It was demonstrated that the ferroelectric domain switching induced by a scanning probe microscopy tip exhibits a rich pattern dynamics, including the intermittency, quasiperiodicity, and chaos. These effects are due to the interplay between the tip-induced polarization switching and the screening charge dynamics and can be mapped onto a logistic map [5]. Using Piezoelectric Force Microscopy (PFM), McGilly *et al.* [6] showed the control and manipulation of domain walls in ferroelectric thin films.

Extra broad domain walls with width about 10–100 nm were observed at the LiNbO$_3$ surface by PFM [7]. On addition, the recent experimental results btained with the use of scanning nonlinear dielectric microscopy (SNDM) [8]·[9] revealed that the wall width near the surface is several times (up to five) higher than in the bulk of thin films of LiTaO$_3$.

The effect of surface wall broadening in ferroelectrics was attributed to the formation of a double electric layer break at the wall-surface junction [10,

11]. However, this mechanism is specific to the domain walls in ferroelectrics with polarization having component normal to the surface [12].

In the case of ferroelastics, the surface effect on elastic twins in a proper ferroelastic was studied in details by Salje *et al.* [13–15]. It was found [14] that the nonzero internal stress exists at a domain wall due to a coupling between the primary order parameter (shear strain) and dilatation strains. The relaxation of stress normal components at the free surface led to either the wall widening or narrowing near the surface depending on the surface curvature sign. Then the electronic phenomena and structure of the twin domain wall – surface junctions in the ferroelastics have been analyzed, by using the example of CaTiO$_3$.

Rychetsky [16] considered the internal stresses occurring around domain walls and showed that the stress can cause a deformation of the crystal surface. The surface distortions have been calculated in the case of antiphase boundaries in tetragonal crystals.

The goal of the paper is to consider the influence of a built-in surface field on the antiparallel 180°-domain wall profile in primary ferroics within the Landau–Ginsburg–Devonshire (LGD) phenomenological approach [17–19]. The built-in surface field causes the phase transition smearing in thin films [20, 21] and stimulates the nucleation of domains during the polarization reversal [22]. This field could be related to either spontaneous symmetry breaking [21, 22] or a misfit between strains of the film and the substrate [20] via the surface piezoelectric effect [23, 24].
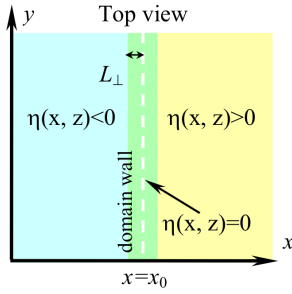
Fig. 1. 180°-domain wall near the sample surface $z = 0$. Order parameter $\eta(x, z)$ has different signs in different domains. Bulk domain wall profile is $x = x_0$

2. Theoretical Formalism

To study the influence of the surface effects on the domain wall itself, we choose the problem geometry for a ferroelectric or ferromagnetic *without depolarization* or *demagnetization fields*, which is possible, e.g., for in-plain components of the order parameter, depending only on coordinates normal to the order parameter (so that the divergence of the order parameter vector is zero, div($\boldsymbol{\eta}$) = 0, and sources of a depolarization field is absent). Note that, for antiferromagnetics or antiferroelectrics, the inhomogeneity of order parameters does not produce any conjugated field, causing a decrease in the order parameter.

The geometry of the problem is presented in Fig. 1. In this case, the polarization (magnetization) pointed along the y-axis do not produce a depolarization (demagnetization) field.

In the case of primary ferroics, the LGD expansion of the bulk Gibbs free energy in powers of the order parameter η (components of the polarization, magnetization, or strain tensor for ferroelectric, ferromagnetic, or ferroelastic media, respectively) is as follows:

$$G_V = \int\limits_{V} d^3r \left(\frac{\alpha}{2}\eta^2 + \frac{\beta}{4}\eta^4 + \frac{\gamma}{2}\left(\frac{\partial \eta}{\partial z}\right)^2 + \right.$$

$$\left. + \frac{\xi}{2}\left(\left(\frac{\partial \eta}{\partial y}\right)^2 + \left(\frac{\partial \eta}{\partial x}\right)^2 \right) \right). \tag{1a}$$

Hereinafter, we neglect the coupling with elastic stresses (i.e., magnetostriction and electrostriction terms). The coefficient $\alpha \sim (T - T_C)$ linearly depends on the temperature T, so that it is negative below Curie temperature T_C. Constants γ and ξ determine the gradient energy strength. Coefficients of the energy expansion β, γ, and ξ are positive and may weakly depend on the temperature.

In the phenomenological theory framework, the surface effects should be taken into account by introducing the surface energy depending on the order parameter as follows:

$$G_S = \int\limits_{S} d^2r \left(\frac{\alpha_S}{2}\eta^2 - \sigma\,\eta \right). \tag{1b}$$

The expansion coefficient α_S is assumed positive (otherwise, higher expansion terms should be considered). The built-in surface field σ may be caused by different physical mechanisms for ferroelastic, ferroelectric, and antiferromagnetic media.

For instance, σ is a component of the intrinsic surface stress tensor for a ferroelastic with order parameter as a component of the strain tensor u_{ij}. Namely, in this case, the surface energy can be rewritten as $\int_S \left(\alpha^S_{ijkl} u_{ij} u_{kl}/2 + \xi_{ij} u_{ij} \right) d^2r$. Here, the summation over repeated indices is assumed, and ξ_{ij} is the intrinsic surface stress tensor [26–28]. It should be noted that, for flat surfaces, only the in-plain components of ξ_{ij} would be invariant under in-plain rotations. Thus, only the in-plain components of the stress could be induced by the surface stress effect.

For the ferroelectrics with order parameter η as a component of the polarization vector P_i, σ originates from the symmetry breaking near the surface. For instance, in the case of a polarization normal to the film surface, vanishing the inversion center leads to the appearance of σ (see, e.g., [20, 21]). In this case, one can write the surface energy as $\int_S (\alpha^S_{ij} P_i P_j/2 + bP_l n_l + \mu_{ijkl} u_{ij} P_k n_l) d^2r$. Here, n_i are components of the normal to the surface, the second term is responsible for the surface local electric field oriented perpendicularly to the surface [20, 21]. The latter term is related to the surface flexoelectric effect [23, 24]. Using the symmetry of the bulk flexoelectric effect for cubic materials [29, 30], it is easy

to estimate that these terms couple in-plain polarization components to shear strains. Although these shear strains are hardly induced by surface stresses, they may appear due to a reconstruction of the surface [31] or the influence of an interface material.

It should be noted that, in the case of a ferromagnetic or superconductor order parameter, the built-in surface field coupled to the corresponding order parameter could not be considered, since the surface could eliminate the symmetry elements corresponding to spatial symmetry but it cannot eliminate the time-reversal or gauge transformations which change ferromagnetic and superconducting order parameters [21]. However, the situation with antiferromagnetic media is more complex, since the allowed symmetry groups for an antiferromagnetic may not include the time-reversal operation, and, thus, these media may possess the piezomagnetic effect [17], as well as terms in the surface energy linear in the order parameter.

One can conclude from the above consideration that, for many different type ferroics media, the appearance of terms linear in the order parameter in the surface energy is quite possible. Here, we consider the impact of these terms on the surface structure of ferroic domain walls.

For the second-order phase transitions considered hereinafter, the LGD equation for the order parameter $\eta(x, z)$ has the form

$$\alpha\eta + \beta\eta^3 - \gamma\frac{\partial^2\eta}{\partial z^2} - \xi\left(\frac{\partial^2\eta}{\partial x^2} + \frac{\partial^2\eta}{\partial y^2}\right) = 0. \qquad (2a)$$

Further, let us consider the case of semiinfinite sample with surface $z = 0$. The inhomogeneous boundary condition for the order parameter is:

$$\left(\eta - \lambda\frac{\partial\eta}{\partial z}\right)\bigg|_{z=0} = \eta_t(x). \qquad (2b)$$

Here, $\lambda = \gamma/\alpha_S$ is the extrapolation length (see, e.g., [32–32]), and the built-in surface order parameter is directly proportional to the surface field as $\eta_t(x, y) = \sigma(x, y)/\alpha_S$.

3. Analytical Results and Discussion

The bulk 1D-solution for a $180°$-domain wall is $\eta_0(x) = \eta_S\tanh((x - x_0)/2L_\perp)$, where the correlation length $L_\perp = \sqrt{-\xi/2\alpha}$ and the spontaneous value $\eta_S^2 = -\alpha/\beta$. It is no more a solution of system (2) in the case $|\lambda| < \infty$.

In the typical case $|\eta_t| < \eta_S$, a linearized solution of Eqs. (2) can be found as $\eta(x, z) = \eta_S\tanh\left(\frac{x-x_0}{2L_\perp}\right) + p(x, z)$, where the perturbation $p(x, z)$ satisfies the inhomogeneous boundary problem:

$$\left(-2\alpha + 3\alpha\,\mathrm{sech}^2\left(\frac{x - x_0}{2L_\perp}\right)\right)p - \gamma\frac{\partial^2 p}{\partial z^2} - \xi\frac{\partial^2 p}{\partial x^2} = 0, \quad (3a)$$

$$\left(p - \lambda\frac{\partial p}{\partial z}\right)\bigg|_{z=0} = \eta_t(x) - \eta_S\tanh\left(\frac{x - x_0}{2L_\perp}\right). \qquad (3b)$$

Here, the hyperbolic function definition $\mathrm{sech}^2(x) = 1 - \tanh^2(x)$ was used.

Looking for a solution of Eqs. (3) in the form $p(x, z) = \int_{k\geqslant 0} dk\, q(k, x)\exp(-kz)$, one obtains the equations for the spectrum $q(k, x)$:

$$\left(-2\alpha + 3\alpha\,\mathrm{sech}^2\left(\frac{x - x_0}{2L_\perp}\right) + \gamma\, k^2\right) \times$$
$$\times q(k, x) - \xi\frac{d^2}{d\, x^2}q(k, x) = 0, \qquad (4)$$

and Eq. (4) is a linear inhomogeneous equation with x-dependent coefficient. The solution of the homogeneous equation for $q(k, x)$ was derived, as proposed in [35], namely:

$$q(k, x) = A(k)f(k, x - x_0) + B(k)f(k, x_0 - x), \qquad (5)$$

$$f(k, x) = \exp\left(i\kappa(k)\frac{x}{2L_\perp}\right) \times$$
$$\times\left(\kappa^2(k) - 2 + 3\mathrm{sech}^2\left(\frac{x}{2L_\perp}\right) + 3i\kappa(k)\tanh\left(\frac{x}{2L_\perp}\right)\right). \quad (6)$$

Then one obtains the integral equation for $A(k)$ and $B(k)$ from the boundary conditions (3b). In the particular case where $\eta_t = $ const, the following approximate analytical solution was derived (see supplementary materials):

$$\eta(x, z) \approx \eta_S\left(1 - \frac{\exp(-z/L_z)}{1 + \lambda L_z}\right) \times$$
$$\times \tanh\left(\frac{x - x_0}{2L_\perp}\right) + \eta_t\frac{\exp(-z/L_z)}{1 + \lambda/L_z}. \qquad (7)$$

By definition, $L_\perp = \sqrt{-\xi/2\alpha}$, $L_z = \sqrt{-\gamma/2\alpha}$. The first term in Eq. (7) is the bulk solution, but with the amplitude depending on the depth due to a diminution of the order parameter on the surface (extrapolation length effect), the second term is due to the
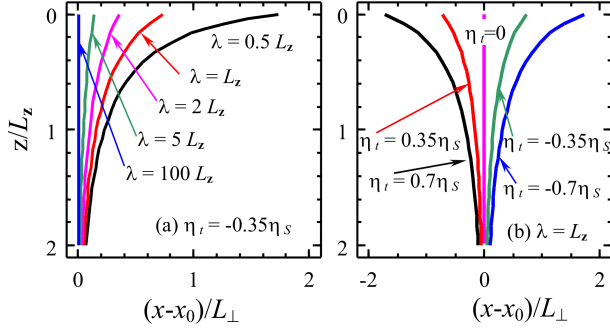
Fig. 2. (Color online) Domain wall profiles (curves $\eta(x,z) = 0$) (*a*) for various extrapolation length λ values (marked near the curves in L_z units) and the built-in field $\eta_t = -0.35\eta_S$; (*b*) for different ratio η_t/η_S values (0, ±0.35, ±0.7) and $\lambda = L_z$. Depending on the sign, the built-in field tends to re-polarize the "left" or "right" surface region and, thus, to bend the domain wall. Bulk ($z \gg L_z$) domain wall profile is $x = x_0$
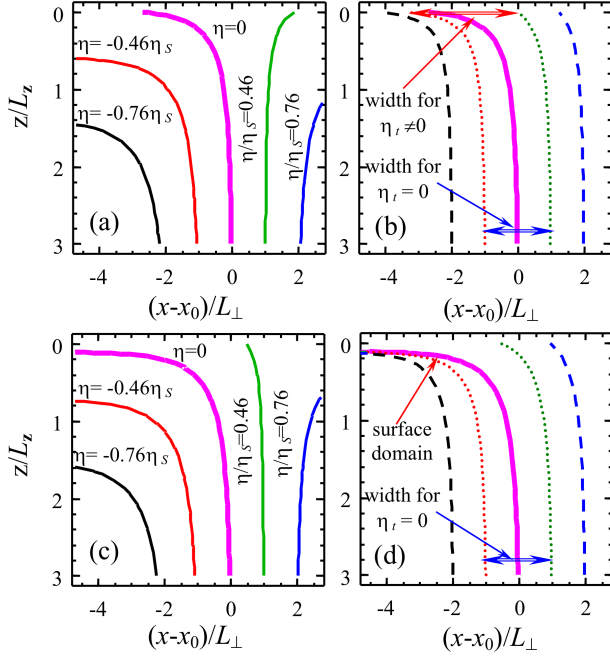
Fig. 3. (Color online) Schematics of the order parameter spatial distribution for $\eta_t = 0.35\eta_S$ (panels (*a*) and (*b*)) and $\eta_t = 0.55\eta_S$ (panels (*c*) and (*d*)). Left column (panels (*a*) and (*c*)) represents map contours of order parameter constant values marked near curves; the curves of fixed width at the levels $\zeta = \pm0.76$ (dashed curves) and ±0.46 (dotted curves) right column (panels (*b*) and (*d*))

built-in surface field. Solution (7) reproduces both the bulk domain wall far from the surface ($z \to \infty$) and the qualitative behavior of the order parameter at the

surface far from the domain wall (and even the quantitative one at high values of λ).

The domain wall position corresponding to Eq. (7) is given by the expression

$$x(z) \approx x_0 - 2L_\perp \times$$
$$\times \operatorname{arctanh}\left(\frac{\eta_t}{\eta_S}\frac{\exp(-z/L_z)}{1 + \lambda L_z - \exp(-z/L_z)}\right). \quad (8)$$

In the case $|\eta_t| < \eta_S\lambda/L_z$, the wall reaches the surface $z = 0$, while, for $|\eta_t| > \eta_S\lambda/L_z$, the built-in surface field induces an ordered surface state instead of the wall bending. Equations (7)–(8) describe the effect of 180°-domain wall bending near the surface as demonstrated in Fig. 2.

Note that the surface state formation in the field of a defect was described earlier [36] for ferroelectric media.

The built-in surface field not only bends the wall, but also leads to changes in a domain wall structure as whole. As one can see from Figs. 3, *a* and 3, *c*, the structure of the wall becomes asymmetric near the surface, and, at sufficiently high values of build-in field, the domain wall could not reach the surface. Moreover, the domain wall width also undergoes changes due to the surface field. It should be noted that the width of a domain wall is usually determined as the distance between the points, where the order parameter reaches a definite fraction of the order parameter value far from the wall (hence, the width determination level).

In our case, the order parameter depends on the z-coordinate even far from the wall (and so does the level). Thus, the width cannot be simply deduced from the contour maps like Figs. 3, *a* and 3, *c*. So, in order to illustrate the dependence of the wall width on the surface field, we calculated the curves, at which the order parameter is equal to a fixed ratio ζ (level) of the order parameter far from the wall but on the same depth, $\eta(x,z) = \pm\zeta\eta(x \to \pm\infty,z)$ (see Fig. 3, *b* and 3, *d*).

The levels about 0.46 and 0.76 are chosen because $\tanh(0.5) \approx 0.46$ and $\tanh(1) \approx 0.76$, so that the width on the level 0.46 is very close to the value $2L_\perp$ for bulk walls.

It is seen from Figs. 3, *b* and 3, *d* that the wall width at the surface increases with η_t and formally reaches infinity, when the near-surface region transforms in the single-domain state.

It is clear that the smaller the extrapolation length λ and/or the higher the ratio $|\eta_t/\eta_S|$, the stronger is the bending effect. Under the absence of a built-in surface field, the domain wall bending or broadening *is absent*, as anticipated in the linear approximation.

The calculated domain wall bending is caused by the nonzero surface field of constant sign. Actually, the built-in surface field distribution may be random (cf. discussion in [22]). Some antisymmetric distribution of the field like $\eta_t \sim \sigma \sim (x - x_0)$ should lead to the pure broadening effect. In addition, the coordinate-dependent surface field with variable polarity could lead to the wall pinning in a weak external field, since the surface field would either promote the nucleation of new domains [22] or, as shown above, would lead to the formation of surface domains in the regions with the opposite value of order parameter. Thus, the external field will "push" the walls to the positions, where $\eta_t \sim \sigma$ is close to zero. However, in a weak external field, the asymmetric surface field would create a restoring force preventing a further displacement of the walls.

For typical material parameters, L_z values are about several lattice constants for ferroelectrics and much higher (up to hundred lattice constants) for magnetics. Scanning probe methods like PFM or SNDM measure the *effective domain wall width* in ferroelectrics, since the probe field penetrates in the depth of the sample at distances 1–10 nm, and so could recognize the bended walls as broadened ones. Thus, the built-in surface field is one of the possible mechanisms of domain wall broadening near the ferroic surfaces.

4. Conclusion

We have considered the influence of the built-in surface field on the 180-degree domain wall profile in primary ferroics within the Landau–Ginsburg–Devonshire phenomenological approach and derived the corresponding approximate analytical expressions. The effect of domain wall bending near the surface caused by the built-in field is predicted. In this case, the higher the surface energy contribution (i.e., the smaller is the corresponding extrapolation length) and/or the higher the field, the stronger is the bending effect. Hence, we can conclude that the built-in surface field is one of the possible mechanisms of domain wall near surface broadening recently observed in the ferroics.

SUPPLEMENTARY MATERIAL

Looking for a solution of Eqs. (3) in the form $p(x, z) = \int_{k \geqslant 0} dk\, q(k, x) \exp(-kz)$, one obtains the equations for the spectrum $q(k, x)$:

$$\left(-2\alpha + 3\alpha \operatorname{sech}^2\left(\frac{x - x_0}{2L_\perp}\right) + \gamma k^2\right) \times$$

$$\times q(k, x) - \xi \frac{d^2}{dx^2} q(k, x) = 0, \tag{S.1a}$$

$$\int_{k \geqslant 0} dk(1 + \lambda k) q(k, x) = \eta_t(x) - \eta_S \tanh\left(\frac{x - x_0}{2L_\perp}\right). \tag{S.1b}$$

Equation (S.1a) is a linear inhomogeneous equation with x-dependent coefficient. The solution of the homogeneous equation for $q(k, x)$ was derived, as proposed in [35], namely:

$$q(k, x) = A(k) f(k, x - x_0) + B(k) f(k, x_0 - x), \tag{S.2a}$$

$$f(k, x) = \exp\left(i\kappa(k)\frac{x}{2L_\perp}\right)\left(\kappa^2(k) - 2 + \right.$$

$$\left. + 3\operatorname{sech}^2\left(\frac{x}{2L_\perp}\right) + 3i\kappa(k)\tanh\left(\frac{x}{2L_\perp}\right)\right). \tag{S.2b}$$

Here, $A(k)$ and $B(k)$ are arbitrary functions of k, the dispersion law $\kappa(k) = 2\sqrt{\frac{L_\perp^2}{\xi} k^2 \gamma - 1}$, while $k \geqslant \sqrt{\xi/\gamma} \cdot L_\perp^{-1}$. Then one obtains the integral equation for $A(k)$ and $B(k)$ from the boundary condition (S.1b) as

$$\int_{k \geqslant 0} dk(1 + \lambda k)\left(A(k) f(k, x - x_0) + \right.$$

$$\left. + B(k) f(k, x_0 - x)\right) = \eta_t(x) - \eta_S \tanh\left(\frac{x - x_0}{2L_\perp}\right). \tag{S.3}$$

Equation (S.3) should be valid at arbitrary x. It reduces to two Fredholm equations of the second order. Only numerical solutions are available.

Without built-in field, $\eta_t = \sigma = 0$, one obtains from Eq. (S.3) that $A(k) = -B(k) = -\eta_S \delta(k - k_0)/(6i\kappa(k))$, $\delta(k)$ is the Dirac-delta function and $k_0 = \sqrt{\xi\gamma} \cdot L_\perp^{-1}$. Finally, the linearized solution acquires the simplest form:

$$\eta(x, z) = \eta_S\left(1 - \frac{\exp(-z/L_z)}{1 + \lambda/L_z}\right)\tanh\left(\frac{x - x_0}{2L_\perp}\right). \tag{S.4}$$

As anticipated, in the absence of a built-in surface field ($\eta_t = 0$), the domain wall bending or broadening *is absent* in the linear approximation.

1. G. Catalan, J. Seidel, R. Ramesh, and J.F. Scott, Rev. Mod. Phys. **84**, No. 1, 119 (2012).
2. Y. Gu, M. Li, A.N. Morozovska, Yi Wang, E.A. Eliseev, V. Gopalan, and L.-Q. Chen, Phys. Rev. B **89**, 174111 (2014).
3. D. Lee, R.K. Behera, P. Wu, H. Xu, S.B. Sinnott, S.R. Phillpot, L.Q. Chen, and V. Gopalan, Phys. Rev. B **80**, 060102(R) (2009).

4. R.K. Behera, C.-W. Lee, D. Lee, A.N. Morozovska, S.B. Sinnott, A. Asthagiri, V. Gopalan, and S.R. Phillpot, J. Phys.: Cond. Matter **23**, 175902 (2011).

5. A.V. Ievlev, S. Jesse, A.N. Morozovska, E. Strelcov, E.A. Eliseev, Y.V. Pershin, A. Kumar, V.Ya Shur, and S.V. Kalinin, Nature Phys. **10**, 59 (2014).

6. L.J. McGilly, P. Yudin, L. Feigl, A.K. Tagantsev, and N. Setter, Nature Nanotechn. **10**, 145 (2015).

7. L. Tian, A. Vasudevarao, A.N. Morozovska, E.A. Eliseev, S.V. Kalinin, and V. Gopalan. J. Appl. Phys. **104**, 074110 (2008).

8. Y. Daimon and Y. Cho, Jap. J. Appl. Phys. **45**, L1304 (2006).

9. Y. Daimon and Y. Cho, Appl. Phys. Lett. **90**, 192906 (2007).

10. E.A. Eliseev, A.N. Morozovska, S.V. Kalinin, Y.L. Li, J. Shen, M.D. Glinchuk, L.-Q. Chen, and V. Gopalan, J. Appl. Phys. **106**, 084102 (2009).

11. The formation of a layer is related to the finite distance between the layers of screening charge and bond charges due the presence of either dead layer or intrinsic size effects.

12. E.A. Eliseev, A.N. Morozovska, Y. Gu, Albina Y. Borisevich, L.-Q. Chen, V. Gopalan, and S.V. Kalinin, Phys. Rev. B **86**, 085416 (2012).

13. J. Novak and E.K.H. Salje, J. Phys.: Cond. Matter **10**, L359 (1998).

14. W.T. Lee, E.K.H. Salje, and U. Bismayer, J. Phys.: Cond. Matter **14**, 7901 (2002).

15. W.T. Lee, E.K.H. Salje, and U. Bismayer, Phys. Rev. B **72**, 104116 (2005).

16. I. Rychetsky, J. Phys.: Cond. Matter **9**, 4583 (1997).

17. L.D. Landau, L.P. Pitaevskii, and E.M. Lifshitz, *Electrodynamics of Continuous Media* (Butterworth-Heinemann, Oxford, 1984).

18. M.E. Lines and A.M. Glass, *Principles and Applications of Ferroelectrics and Related Phenomena* (Clarendon Press, Oxford, 1977).

19. Ch. Kittel, *Introduction to Solid State Physics* (Wiley, New York, 1974).

20. M.D. Glinchuk and A.N. Morozovska, J. Phys.: Cond. Matter **16**, 3517 (2004).

21. A.M. Bratkovsky, and A.P. Levanyuk, Phys. Rev. Lett. **94**, 107601 (2005).

22. G. Gerra, A.K. Tagantsev, and N. Setter, Phys. Rev. Lett. **94**, 107602 (2005).

23. A.P. Levanyuk and S.A. Minyukov, Sov. Phys. Solid State **25**, 2007 (1983).

24. A.K. Tagantsev, Phys. Rev. B **34**, 5883 (1986).

25. A. Hubert and R. Schafer, *Magnetic Domains: The Analysis of Magnetic Microstructures* (Springer, Berlin, 1998).

26. V.I. Marchenko, and A.Ya. Parshin, Sov. Phys. JETP **52**, 129 (1980).

27. V.A. Shchukin and D. Bimberg, Rev. Mod. Phys. **71**, 1125 (1999).

28. Y. F. Gao and Z. Suo, J. of Appl. Mech. **69**, 419 (2002).

29. G. Catalan, L.J. Sinnamon, and J.M. Gregg, J. Phys.: Cond. Matter **16**, 2253 (2004).

30. P. Zubko, G. Catalan, A. Buckley, P.R. Welche, and J.F. Scott, Phys. Rev. Lett. **99**, 167601 (2007).

31. K. Oura, V.G. Lifshits, A.A. Saranin, A.V. Zotov, and M. Katayama, *Surface Science: An Introduction* (Springer, Berlin 2003).

32. M.I. Kaganov and A.N. Omelyanchouk, Sov. Phys. JETP **34**, 895 (1972).

33. R. Kretschmer and K. Binder, Phys. Rev. B **20**, 1065 (1979).

34. C.-L. Jia, V. Nagarajan, J.-Q. He, L. Houben, T. Zhao, R. Ramesh, K. Urban, and R. Waser, Nature Mat. **6**, 64 (2007).

35. R.K. Dodd, J.C. Eilbeck, J.D. Gibbon and H.C. Morris, *Solitons and Nonlinear Wave Equations* (Academic Press, London, 1984).

36. A.N. Morozovska, S.V. Svechnikov, E.A. Eliseev, B.J. Rodriguez, S. Jesse, and S.V. Kalinin, Phys. Rev. B **78**, 054101 (2008).

Є.А. Єлісеєв

СТРУКТУРА 180-ГРАДУСНОЇ ДОМЕННОЇ
СТІНКИ ПОБЛИЗУ ПОВЕРХНІ ФЕРРОЇКІВ

Р е з ю м е

Розглянуто вплив вбудованого поверхневого поля на профіль 180 градусної доменної стінки у власних ферроіках в рамках феноменологічного підходу Ландау–Гінзбурга–Девоншира. Вбудоване поверхневе поле може бути створене різними фізичними механізмами в сегнетоеластичних, сегнетоелектричних і антиферомагнітних середовищах. Наприклад, це може бути компонента тензора поверхневих напружень для сегнетоеластиків з відповідним параметром порядку, компонентами тензора деформації. Передбачений ефект вигину доменної стінки поблизу поверхні, викликаний вбудованим полем, і отримані відповідні наближені аналітичні вирази для його опису.